J. Astrophys. Astr. (1980) **1,** 17–23

Lines formed in Rotating and Expanding Atmospheres

A. Peraiah *Indian Institute of Astrophysics, Bangalore* 560034

Received 1980 February 23; accepted 1980 April 7

Abstract. Spectral lines formed in a rotating and expanding atmosphere have been computed in the frame of the observer at infinity. Two kinds of velocity laws are employed: (i) a uniform radial velocity of the gas and (ii) velocity increasing with radius (*i.e.* velocity gradients). The atmosphere has been assumed to be rotating with constant velocity. We have considered maximum radial and rotational velocities to be 10 and 3 mean thermal units respectively in an atmosphere whose geometrical thickness is 10 times the stellar radius. The total radial optical depth at line centre is taken to be about 100. In all cases, Doppler profile and a source function which is varying as $1/r^2$ have been used.

Generally, the lines are broadened when rotation is introduced. However, when radial motion is also present, broadening becomes asymmetric and the red emission and blue absorption are enhanced.

Key words: rotating and expanding atmospheres—spectral lines—radiative transfer—P Cygni profiles

1. Introduction

Rotation is a common phenomenon among all the celestial objects. The stellar rotation is evidenced in the broadening of the spectral lines formed in their atomspheres. The rotational aspects of the rings of Be stars are discussed in Slettebak (1979). However, we should consider systems in which the atmosphere is rotating. In addition to rotation, the radial motion of the gas in the atmosphere is also an important factor which could change the shape of the spectral lines. Recently, several methods of calculating spectral lines in a radially moving gas have been developed (see Mihalas 1978; Peraiah 1978). However, the combined effects of rotation of the atmosphere and the radial motion of the gases in the atmosphere are not very well understood. Recently, Dural and Karp (1978) calculated lines with these two effects taken into account in a semi-analytical way. However, they used

small velocities of rotation and radial motion with no velocity gradients. They have used the limb darkening law (Gray 1976) to calculate the specific intensities.

In this paper, we compute spectral lines seen by the observer at the earth by using the formal solution of the radiative transfer equation for a medium with radial optical depth of 100 at the line centre, using a maximum rotational velocity of 3 and radial velocity of the gas of 10 mean thermal units. The results are presented in the next section.

2. Computational procedure and discussion of results

The geometry of the calculations is given in Fig. 1. The medium has been divided into several shells. The rotational velocity $V_{\rm rot}$ and the radial velocity $V_{\rm rad}$ at each point on the shells are projected on to the line of sight 1 of the observer. So, the resultant frequency is given by

$$x = x' + \mathbf{v}_{\rm rot} \cdot \mathbf{l} + \mathbf{v}_{\rm rad} \cdot \mathbf{l}, \tag{1}$$

where $x' = (\nu' - \nu_0)/\Delta\nu_D$, $\Delta\nu_D = v_T(\nu_0/c)$.

$\mathrm{v}_{\rm rot}$ and $\mathrm{v}_{\rm rad}$ are measured in units of v_T , the mean thermal velocity of the gas. The atmosphere has been divided into several shells as shown in Fig. 1. The optical depth is calculated in each of these shells along the line of sight after taking into

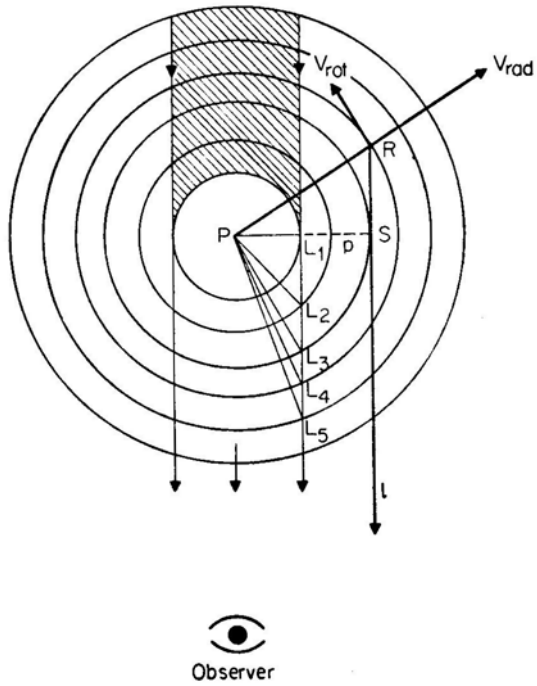

Figure 1. Diagram showing the stellar disc from which radiation is received at infinity.

account the projection of v_{rot} and v_{rad} on to 1 and is given by

$$\tau_L = \frac{\pi e^2}{mc} f \frac{\Delta L}{\Delta \nu_D \sqrt{\pi}} N \exp(-x^2/\delta^2), \tag{2}$$

where ΔL is the length along the ray between two consecutive shell boundaries (L_1L_2 or L_2L_3 etc.) and $\delta = \Delta^{\nu}{}_D(r)/\Delta^{\nu}{}_D$, the ratio of the Doppler widths, is kept equal to. 1. We calculate the transfer of the rays along the line of sight. These are parallel rays cutting across the shell boundaries. N is the particle density. The specific intensity at each shell boundary becomes the incident radiation for the transfer of radiation in the next shell. No incident radiation is given at the outermost boundary. The emergent intensity is calculated by the formal solution of radiative transfer equation and is given by

$$I(\tau_L) = I_0 \exp(-\tau_L) + \int_0^{\tau_L} S(t) \exp[-(\tau_L - t)]\, dt, \tag{3}$$

where $S(t)$ is the source function. The radial distribution of the source function is obtained from the solution of the radiative transfer equation in spherical symmetry either in the rest frame of the star or in the comoving frame of the gas. However, as we are investigating the combined effects of rotation and radial motion on the formation of lines qualitatively, we have assumed a source function which varies as $1/r^2$. With this assumption, we can estimate the specific intensity $I(\tau_L)$ at the boundary of each shell. The integral in equation (3) is evaluated by Simpson's rule. Finally we calculate the flux by the integral

$$F(x) = 2\pi \int_A^B I(p, x) p\, dp, \tag{4}$$

where p is the perpendicular distance from the centre of the star P to the ray along the line of sight and A and B are the inner and outer radii of the medium.

We have assumed two types of variations for the velocity satisfying the law of continuity: (i) increasing linearly with radius, *i.e.*

$$V_r = V_A + \frac{V_B - V_A}{B - A}(r - A), \tag{5}$$

where V_A, V_B and V_r are the velocities at A, B and r respectively; and (ii) a constant velocity throughout the atmosphere $V = V_A = V_B$. The density changes as $1/r^3$ in the first case and as $1/r^2$ in the second case such that the equation of continuity is always satisfied. We have assumed constant velocity of rotation in all shells so that the angular velocity changes as $1/r$ (so that angular momentum is conserved on the whole). In the first case, we have set V_A = 0 and V_B =0, 1, 3,6and 10 and V_{rot} = 0, 1 and 3 mean thermal units (mtu) whereas in the second case,

the values of V_{rot} are the same as in case 1 but with V = 0, 1 and 3 mtu only. The inner and outer radii of the atmosphere are taken to be 10^{12} and 10^{13} cm respectively and the density at radius A is put at 10^6 cm^{-3}.

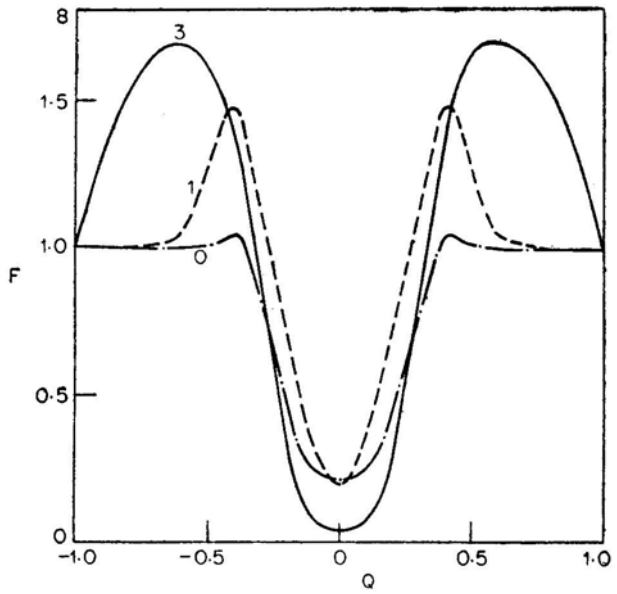

Figure 2. Flux profiles for differential radial velocities with $V_B=V_A=0$ and V_{rot}=0, 1 and 3. $Q=X/X_{max}$ and F=flux (X)/flux (X_{max}). The numbers refer to V_{rot} .

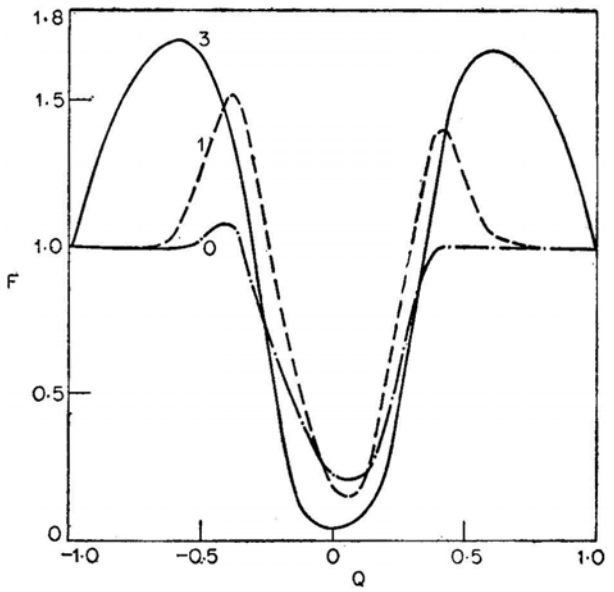

Figure 3. Flux profiles for $V_B=1$, $V_A=0$ and V_{rot} =0, 1, 3.

In Fig. 2 we have plotted flux profiles *i.e.* $F(=F(x)/F(X_{max}))$ versus Q $(=X/X_{max})$for V_B =0 and V_{rot} =0, 1 and 3 mtu. The line for V_{rot} = 0 shows deep absorption but with slight emission (about 5 per cent) in the wings. However, when rotation is introduced, the lines show a large broadened emission of nearly 50 per cent forV_{rot} =1 and 70 per cent for V_{rot} =3 mtu. But the absorption becomes sharper for V_{rot} = 1 and both emission and absorption become broader and deep. When rotation is introduced into the radially moving matter, there will be an artificial extension of the outer layers which means that the side lobes of the atmosphere from which the scattered radiation arrives at the observer, extend and increase the emission.

In Fig. 3 flux profile for V_B=1 mtu and V_{rot}= 0, 1,3 mtu is presented. There is a small red emission for V_{rot} =0 and no emission on the blue side of the centre of the line. However, when rotational velocity is introduced both emission and absorption increase and there is emission on the blue side which is comparable to that on the red side. These features become strong as we increase the radial velo-

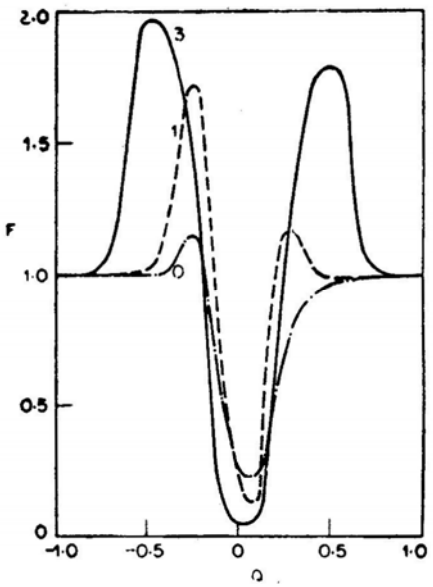

Figure 4. Flux profiles for V_B=3, V_A=0 and V_{rot}=0, 1, 3.

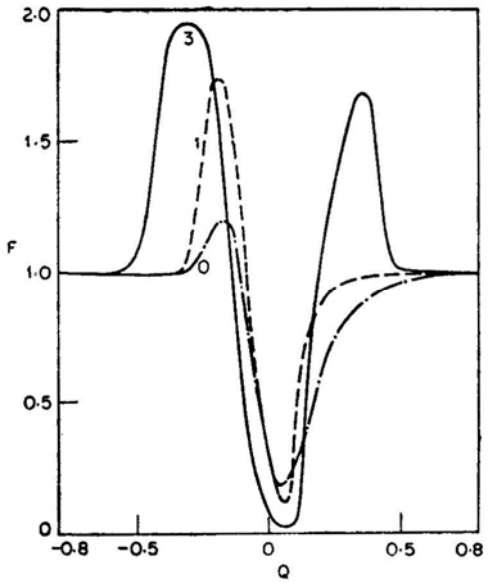

Figure 5. Flux profiles for V_B=6, V_A=0 and V_{rot}=0, 1, 3.

city to 3, 6 and 10 mtu. At V= 10 mtu and V_{rot} = 3, the asymmetry is quite large. These are shown in Figs 4, 5 and 6. In Figs 7 and 8 the flux profiles for the second case (uniform radial motion) are presented. The profiles in Fig. 7 are calculated for V_B =V_A=1 mtu and V_{rot} = 0, 1, 3 mtu. We clearly notice the P Cygni profiles for V_{rot} = 0 and rotation introduces emission in the blue side (compare this with profiles given in Fig. 3). In Fig. 8 we present the profiles for V=3 mtu and V_{rot} = 0, 1, 3 mtu, These profiles exhibit clearly the type of

profiles one would expect from P Cygni atmospheres. As the rotational velocity increases, the red emission becomes larger and its peak becomes redder

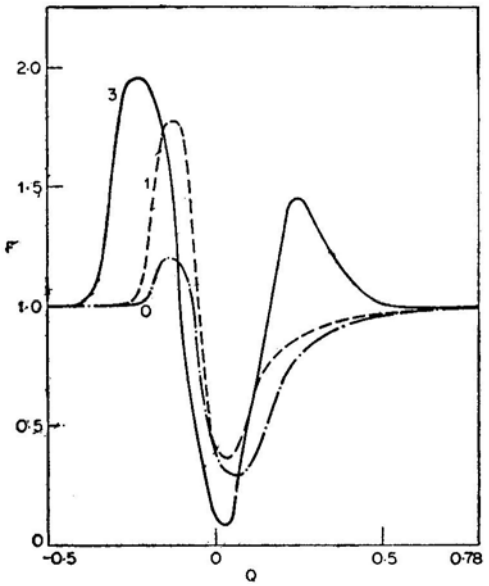

Figure 6. Flux profiles for V_B=10, V_A=0 and V_{rot}=0, 1, 3.

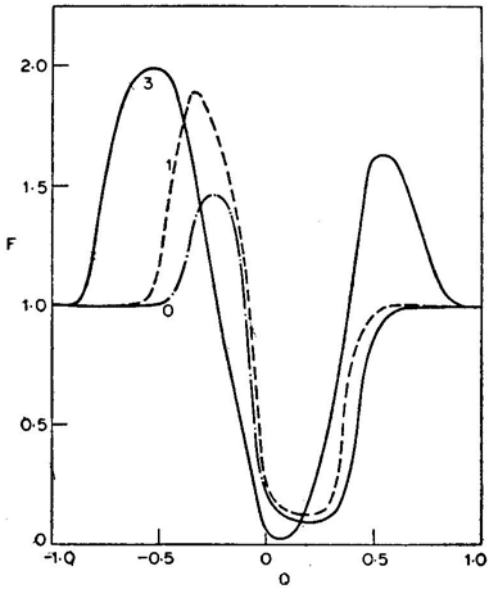

Figure 7. Flux profiles for $V_A = V_B$ =l, V_{rot} =0, **1.**

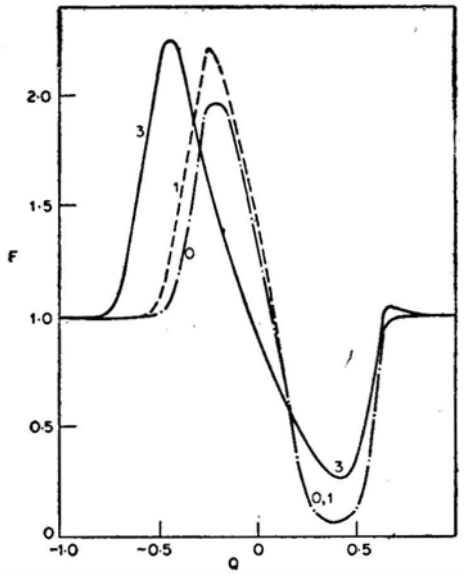

Figure 8. Flux profiles for $V_A = V_B = 3$, $V_{rot} = 0, 1, 3$.

3. Conclusions

The effects of rotational velocities on the formation of spectral lines formed in an atmosphere with radial velocities, have been investigated. Radial motion of the gases introduce a P Cygni type-shape and rotational motion would increase the emission on either side of the centre of the line although the line remains asymmetric.

References

Dural, P., Karp, A. H. 1978, *Astrophys., J.*, **222,** 220.
Gray, D. F. 1976, *The Observations and Analysis of Stellar Photospheres,* John Wiley, New York.
Mihalas, D. 1978, *Stellar Atmospheres,* 2 edn, Freeman, San Francisco.
Peraiah, A. 1978, *Kodaikanal Obs. Bull. Ser. A,* **2,** 115.
Slettebak, A. 1979, *Space Sci. Rev.*, **23,** 541.